Original Article

MOLECULAR PAIN

Molecular Pain
Volume 12: 1–11

DOI: 10.1177/1744806916629051
mpx.sagepub.com
SAGE

Epidural optogenetics for controlled analgesia

Robert P Bonin, PhD[1], Feng Wang, PhD[1], Mireille Desrochers-Couture[1], Alicja Gąsecka, PhD[2], Marie-Eve Boulanger[1], Daniel C Côté, PhD[2] and Yves De Koninck, PhD[1,3]

Abstract

Background: Optogenetic tools enable cell selective and temporally precise control of neuronal activity; yet, difficulties in delivering sufficient light to the spinal cord of freely behaving animals have hampered the use of spinal optogenetic approaches to produce analgesia. We describe an epidural optic fiber designed for chronic spinal optogenetics that enables the precise delivery of light at multiple wavelengths to the spinal cord dorsal horn and sensory afferents.

Results: The epidural delivery of light enabled the optogenetic modulation of nociceptive processes at the spinal level. The acute and repeated activation of channelrhodopsin-2 expressing nociceptive afferents produced robust nocifensive behavior and mechanical sensitization in freely behaving mice, respectively. The optogenetic inhibition of GABAergic interneurons in the spinal cord dorsal horn through the activation of archaerhodopsin also produced a transient, but selective induction of mechanical hypersensitivity. Finally, we demonstrate the capacity of optogenetics to produce analgesia in freely behaving mice through the inhibition of nociceptive afferents via archaerhodopsin.

Conclusion: Epidural optogenetics provides a robust and powerful solution for activation of both excitatory and inhibitory opsins in sensory processing pathways. Our results demonstrate the potential of spinal optogenetics to modulate sensory behavior and produce analgesia in freely behaving animals.

Keywords

Optogenetics, pain, analgesia, spinal cord, dorsal horn, plasticity, optics, allodynia, hyperalgesia

Date received: 2 October 2015; accepted: 18 November 2015

Introduction

Noxious and innocuous sensation is largely mediated through the transmission of sensory information from the periphery to the spinal cord via modality-specific sensory afferents.[1] The precise nature of sensation is dependent not only on the pattern of sensory afferents activated peripherally but also on how this input is processed and integrated in the spinal cord.[2] Abnormalities in either afferent or dorsal horn interneuronal activity can lead to pathological sensory conditions, including chronic pain.[2–4] Deciphering how sensory information is relayed through the spinal cord from the periphery and how this process changes in pathological conditions is crucial for the development of novel therapeutic approaches that treat the root causes of sensory dysfunction.

Optogenetic tools offer a powerful means for the cell-specific, functional dissection and modulation of sensory circuits. Optogenetic proteins have previously been expressed in genetically[5] and biologically defined[6] sensory afferent populations to study nociception induced by peripheral optical stimulation. In vitro studies have also employed optogenetics to explore sensory and

[1]Institut Universitaire en santé mentale de Québec, Québec, Canada
[2]Department of Physics, Université Laval, Québec, Canada
[3]Department of Psychiatry and Neuroscience, Université Laval, Québec, Canada

Corresponding author:
Yves De Koninck, Division of Cellular and Molecular Neuroscience, Institut Universitaire en sante mentale de Québec 2601, Chemin de la Canardiere Québec, QC, G1J 2G3 Canada.
Email: yves.dekoninck@neuro.ulaval.ca

motor circuitry of the spinal cord.[7–11] However, the difficulty in delivering light to the spinal cord of freely behaving animals has hindered the optogenetic study of how spinal processing modulates behavioral responses to sensory input.

Recently, a subcutaneous, wireless light-emitting diode (LED) system was described that could activate channelrhodopsin-2 (ChR2) expressing sensory afferents either peripherally or at the spinal level.[12] This advancement enabled the manipulation of sensory afferents in awake mice. Yet, it is unclear whether this LED approach can deliver sufficiently intense light for the activation of inhibitory optogenetic proteins such as archaerhodopsin (ArchT) that have a higher threshold for activation than channelrhodopsin, or for the activation or inhibition of neurons within sensory processing pathways of the spinal cord dorsal horn that lie beneath a layer of myelin. The inhibition of nociceptive afferents via activation of ArchT or manipulation of intrinsic spinal neuron activity to inhibit the activity of nociceptive projection neurons would enable optogenetic induction of analgesia—one of the key therapeutic possibilities enabled by spinal cord optogenetics.

To overcome this key obstacle, we have developed an effective epidural optic fiber implant for mice that is entirely compatible with conventional LED or laser-based optogenetic systems, and that enables the spinal delivery of light in acute and chronic experiments. This approach offers the advantages of permitting delivery of multiple wavelengths of light for the activation of the complete palette of optogenetic proteins, as well as the delivery of sufficient light intensity for activating or inhibiting intrinsic spinal cord neurons in sensory processing pathways. We used this easily constructed and readily employed design to induce mechanical hyperalgesia arising from sensory plasticity and dorsal horn disinhibition, and the immediate and acute induction of analgesia.

Methods

Animals

All behavioral experiments were conducted in accordance with the guidelines established by the Canadian Council for Animal Care. Adult (>12 weeks old) male C57BL/6 mice were used for experiments except where indicated otherwise. Mice were kept on a 12:12 light:dark cycle in groups of one to four mice per cage prior to fiber implantation, and singly housed after implantation of the fiber, with food and water provided ad libitum. All experiments started prior to 10:00.

Optogenetic mouse models were generated using three different approaches to highlight a number of applications of the epidural optic fiber (see Table 1). Mice expressing ChR2 in $Na_v1.8^+$ nociceptive afferents ($Na_v1.8$-ChR2) were generated by crossing mice expressing Cre-recombinase in $Na_v1.8^+$ neurons ($Na_v1.8$-Cre; generously provided by Rohini Kuner)[13] with mice expressing a loxP-flanked STOP cassette upstream of a ChR2-EYFP fusion gene at the Rosa 26 locus (Rosa-CAG-LSL-ChR2(H134R)-EYFP-WPRE; stock number 012569, The Jackson Laboratory, Bar Harbor, ME). In these mice, Cre expression is restricted to the dorsal root ganglia, and the vast majority (>90%) of Cre-expressing cells are unmyelinated C-fibers that innervate the superficial dorsal horn (Figure 1(a) and (b)).[13,14] Mice expressing ArchT in $Na_v1.8^+$ nociceptive afferents were generated by intraperitoneal injection of neonatal (P5) $Na_v1.8$-Cre mouse pups with 20 µl of AAV8 virus Cre-dependently expressing ArchT (AAV8-CBA-Flex-ArchT-GFP-WPRE-SV40, $>10^{13}$ particles·ml^{-1}, University of North Carolina). We confirmed that this technique efficiently transfects dorsal root ganglia neurons while sparing the spinal cord dorsal horn by injecting neonatal mouse pups (P5) intraperitoneally with with Cre-independent AAV9 expressing GCaMP (AAV9, CAG-GCaMP6s-WPRE-SV40, $>10^{13}$ particles·ml^{-1}, University of Pennsylvania), after which we observed no transfection of spinal cord neurons (Figure 1(c) and (d)).[15] Mice expressing ArchT in spinal cord inhibitory interneurons were generated by intraspinal injection of AAV8 virus Cre-dependently expressing ArchT into adult (eight weeks) male GAD2-IRES-Cre mice (Stock number 010802, The Jackson Laboratory). Briefly, adult mice were anesthetized with 2.5% to 3% isoflurane and L3 through L5 spinal cord was exposed by laminectomy; 500 nl of AAV8-CBA-Flex-ArchT-GFP-WPRE-SV40

Table 1. Summary of optogenetic models and approaches used.

Mouse model	Method of generation	Method of light delivery	Figure
$Na_v1.8$-ChR2	$Na_v1.8$-Cre × Floxed ChR2	Epidural in awake	4b,c,f
$Na_v1.8$-ChR2	$Na_v1.8$-Cre × Floxed ChR2	Peripheral under anesthesia	4d
$Na_v1.8$-ChR2	$Na_v1.8$-Cre × Floxed ChR2	Epidural under anesthesia	4e
GAD2-ArchT	Intraspinal AAV in GAD2-Cre	Epidural in awake	4h,i
$Na_v1.8$-ArchT	I.P. AAV (neonates) in $Na_v1.8$-Cre	Epidural in awake	4k
C57BL/6	None	Epidural in awake	4l

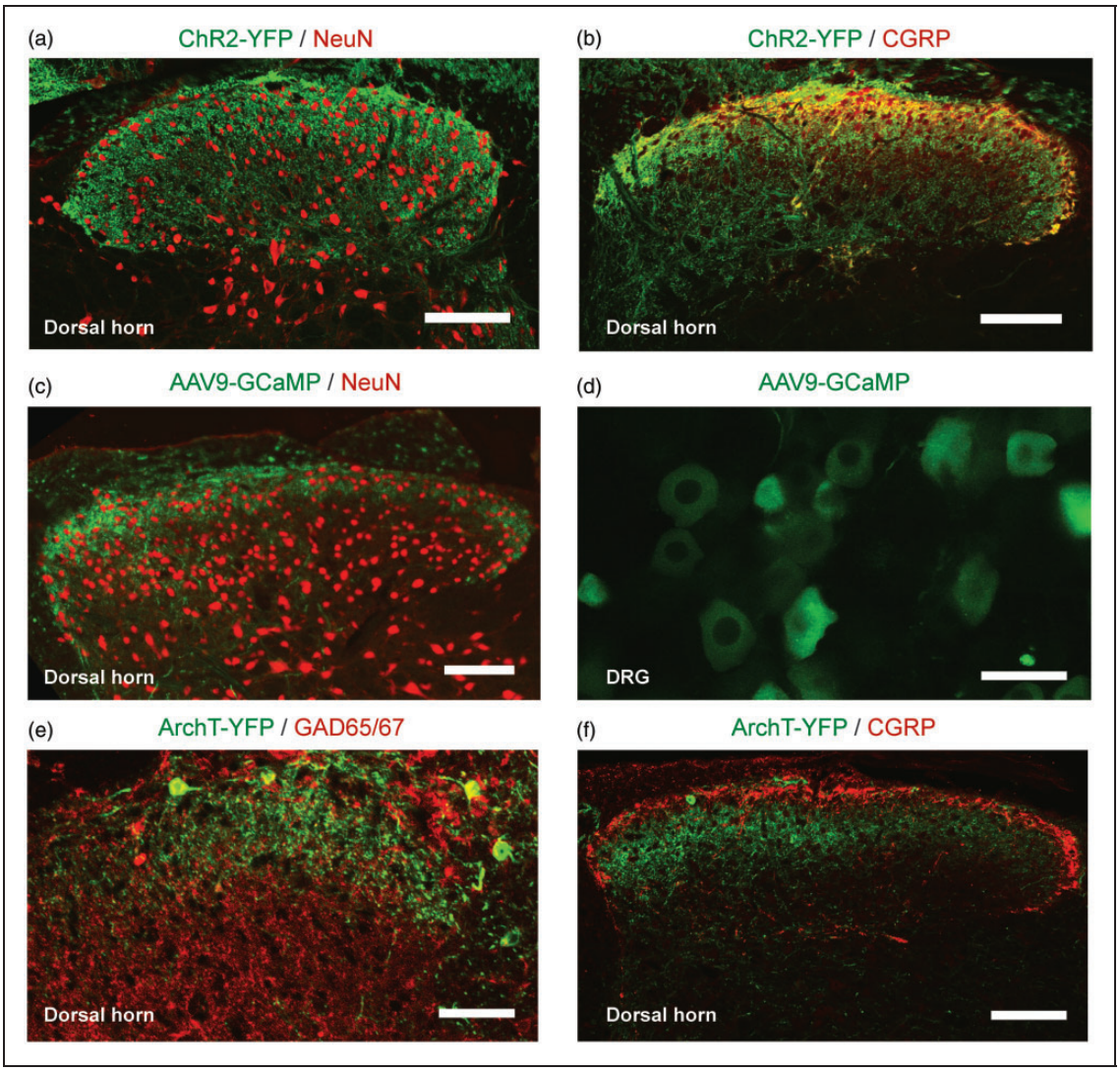

Figure 1. Characterization of optogenetic mouse models used. (a,b) Spinal expression of ChR2-YFP in $Na_v1.8$-ChR2 mice. ChR2-YFP does not colocalize with NeuN (a), and is predominantly present in the superficial dorsal horn (b), consistent with its restricted expression in $Na_v1.8^+$ sensory afferents. (c,d) Expression of GCamP6 as a cellular marker in superficial dorsal horn and dorsal root ganglia neurons after systemic transfection of neonatal mouse pups with GCamP6-expressing AAV9 administered via i.p. injection. GCaMP6 expression is restricted to afferent terminals entering the spinal cord dorsal horn (c) and neurons of the DRG (d), indicating the route of AAV9 virus-administration does not transfect intrinsic dorsal horn neurons. (e) Expression of ArchT-YFP in GAD65/67$^+$ neurons of the dorsal horn after intraspinal injection of Cre-dependent AAV9 expressing ArchT-YFP in GAD2-Cre mice. (f) The expression of ArchT-YFP was largely restricted to the superficial dorsal horn of intraspinallyinjected GAD2-Cre mice. Scale bars of a, b, c, and f indicate 100 μm. Scale bars of d, e indicate 50 μm.

($>10^{13}$ particles·ml^{-1}, University of North Carolina) were pressure ejected into the spinal parenchyma at a depth of 100 μm via a glass pipette connected to a nanoinjector (Micro 4, World Precision Instruments, Florida, USA) at a rate of 100 nl·min^{-1}. The injection was carried out four times bilaterally (two times on each side) on each mouse. The expression of ArchT was restricted to the superficial dorsal horn and overlapped with GAD65/67 expression (Figure 1(e) and (f)). Mice were allowed to recover from intraspinal injection for four weeks prior to epidural fiber implantation.

Epidural fiber production and implantation

The epidural optic fiber implant consisted of a length of multimode plastic fiber (240 μm core, 250 μm diameter with cladding, 0.62 NA) modified with a diffusive tip (Doric Lenses, Quebec, Canada) to enable multidirectional diffusion of light from the fiber (Figure 2(a) and (b); Figure 3(a)). The fiber was fitted with a ceramic ferrule (2.5 mm diameter, 270 μm bore; Thor Labs, Germany) and the length of the fiber from the end of the ferrule to the diffusive tip was typically 40 mm, but

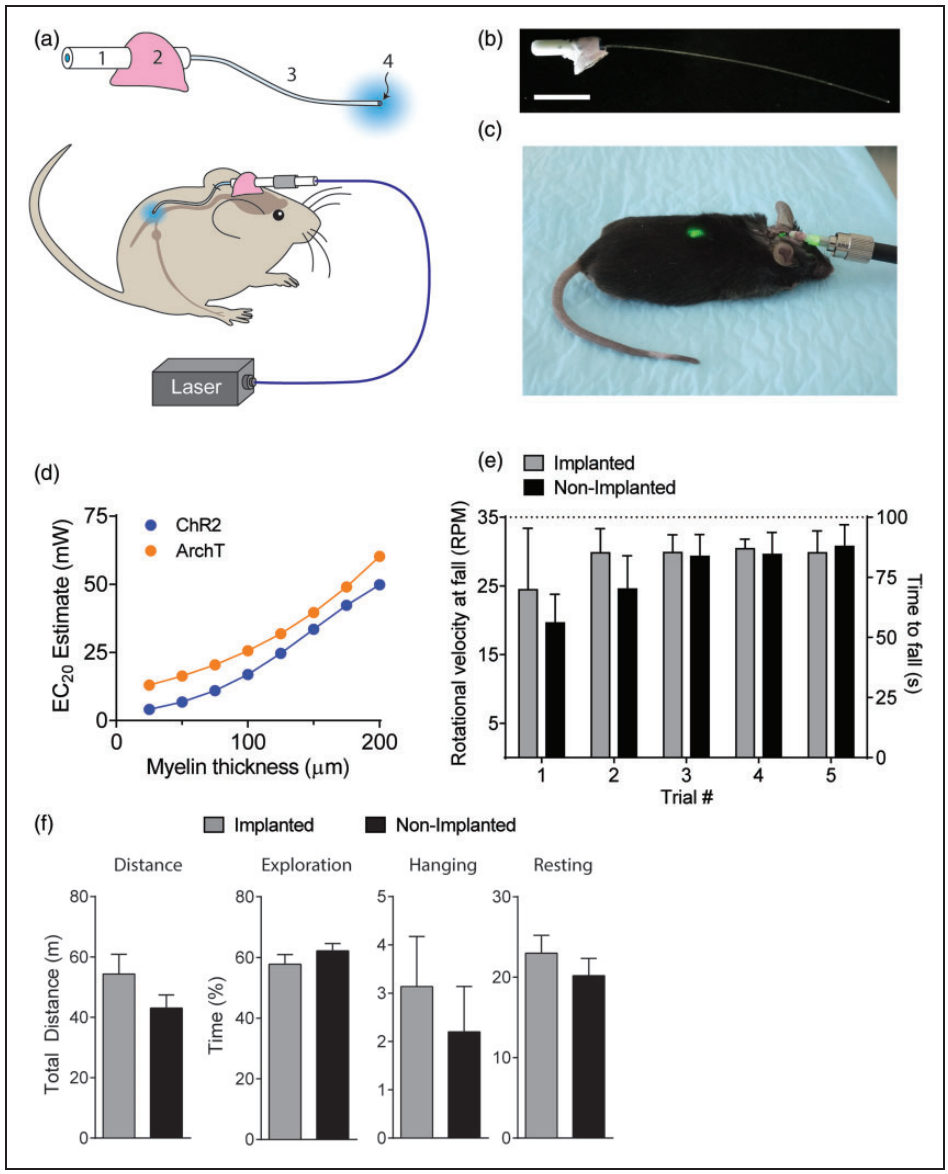

Figure 2. Development and characterization of an epidural optic fiber implant. (a) The epidural optic fiber implant consists of a bare ferrule (1) embedded in a preformed dental cement base that facilitates fixation to the skull (2). The optic fiber (3) connected to the ferrule is a high-aperture, large-diameter core (240 μm) plastic fiber modified with a diffusive tip (4) to enable illumination of the spinal cord ventral to the fiber tip. The optic fiber is epidurally implanted in a mouse and connected to a fiber-coupled laser via a light-weight sleeve. (b) Image of an epidural optic fiber before implantation. Scale bar indicates 1 cm. (c) Image of a mouse immediately after implantation surgery with epidural optic fiber connected directly to a green light source (not to an experiment patch cable) to verify positioning of the fiber tip. (d) Estimation of power output from the diffusive tip of the optic fiber required for activation of opsins in the spinal cord dorsal horn using a threshold of activation (EC_{20}) of 0.3 mW · mm^{-2} and 0.75 mW · mm^{-2} for ChR2 and ArchT, respectively. (e) Motor performance of epidural fiber-implanted and control mice in the RotaRod task. $n = 6$ mice per group. (f) Distance measurement and activity analysis of implanted and non-implanted mice placed in novel cage for 1 h. $n = 6$ mice per group.

varied from 38 mm to 42 mm for implantation in longer or shorter mice, as necessary. A 5 mm diameter base of dental cement was added to the ferrule prior to implantation to facilitate fixation on the skull of the mouse.

Mice were anesthetized with isoflurane (2% to 2.5%) delivered by a flexible tube fitted with a latex nose cone to enable to manipulation of mouse during the surgery. The head and neck of the mice were shaved and a 1.5-cm incision was made from the first vertebrae to the skull. The dorsal neck muscles were separated at midline and retracted with the head held at a downward angle (approximately 45° from parallel) to expose the posterior atlanto-occipital membrane. The atlanto-occipital membrane was vigorously, mechanically cleaned

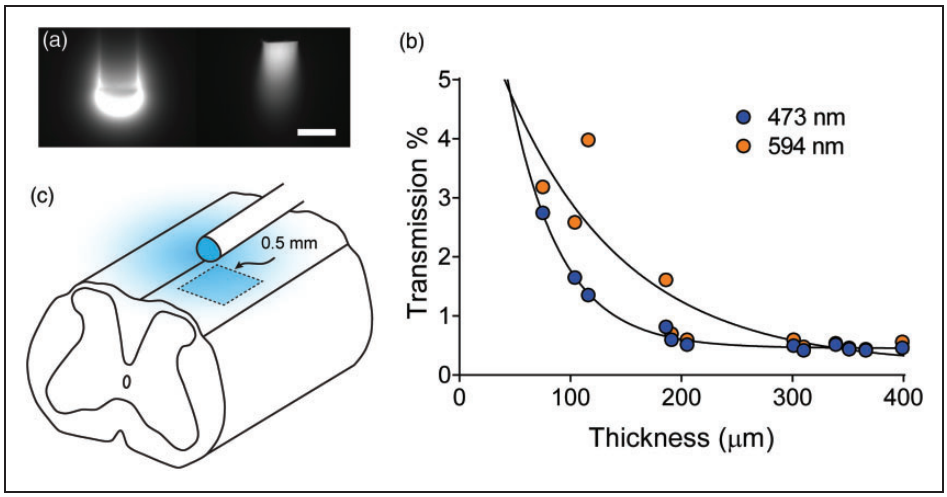

Figure 3. Activation of opsins expressed by sensory afferents and neurons of the spinal cord dorsal horn with a diffusive-tipped epidural optic fiber. (a) A diffusive-tipped optic fiber was used to ensure the ventrally transmission of light towards the dorsal horn. Demonstration of light emission from a diffusive-tipped fiber (left) compared to a standard, non-diffusive-tipped fiber (right), showing a wide angle of light emission from diffusive tip. Both fibers were immersed in a fluorescent FITC solution and injected with blue (473 nm) light. Scale bar indicates 250 μm. (b) Measurement of light transmission through various thicknesses of spinal cord myelin. (c) Schematic drawing of the model used for estimation of the power output from the diffusive tip of the optic fiber required for activation of opsins in the spinal cord dorsal horn (see Methods).

with a cotton swab with particular attention paid to the point of connection to the first vertebrae (C1). This cleaning procedure does not perforate the membrane and promotes separation of the atlanto-occipital membrane from the dura to facilitate the epidural placement of the optic fiber. The optic fiber was carefully inserted through the atlanto-occipital membrane and under C1, immediately rostral to C1, with the head held at an acute, downward angle. Correct insertion was associated with a lack of cerebrospinal fluid loss at the site of insertion. With the head maintained at an acute angle and the body of the mouse suspended off the surgical table, the fiber was carefully inserted along the length of the spinal cord. The mouse was repositioned as necessary to straighten the natural curvature of the spine during implantation. The correct positioning of the fiber tip near L1 (corresponding to spinal segments L4 through L6[16]) was confirmed by connecting the fiber to a light source and observing the illuminated region on the back (Figure 2(c)). Once the fiber was correctly positioned, the skull of the mouse was cleaned with a small quantity of 30% H_2O_2 (Sigma Aldrich, Canada), rinsed thoroughly with saline, and blotted dry. The dental cement base of the fiber was fixed to the skull with Loctite 454 Prism instant adhesive and the incision sutured closed. The implanted mice were allowed to recover from anesthesia and the animals were monitored to ensure a lack of paralysis or movement abnormalities indicative of improper fiber placement before being housed in a standard home cage without environmental enrichment. Mice were allowed to recover from surgery for at least one week prior to experimentation.

Immunohistochemistry

For immunohistochemistry, mice were anesthetized with ketamine/xylazine and transcardially perfused with 4% w/v paraformaldehyde and 0.1% v/v picric acid in phosphate buffer. The spinal cord was dissected and post-fixed for 2 h. Notably, no gross deformation or damage caused by the epidural optic fiber was observed upon spinal cord extraction for immunohistochemistry. The tissue was cryo-protected in 30% sucrose solution overnight and then sectioned by a cryostat at 14 μm thickness. The sections were stained with rabbit antibodies against CGRP (1:2000; C8198, Sigma Aldrich), mouse anti-NeuN antibodies (1:800; MAB377, Chemicon), or rabbit anti-GAD65/67 antibodies (1:200; AB1511, Millipore), followed by incubation with Alexa Fluor 543-conjugated goat secondary anti-rabbit antibodies (1:100; Molecular Probes) or Alexa Fluor 647-conjugated goat secondary anti-mouse antibodies (1:100; Molecular Probes). Sections were examined under an Olympus Fluoview FV1000 confocal laser scanning microscope.

Physical model of spinal cord irradiance

Myelinated spinal cord slices were obtained from adult male C57BL/6 mice. Mice were anesthetized with urethane ($2\,g \cdot kg^{-1}$) and perfused with ice-cold artificial cerebral spinal fluid (aCSF; composition in mM: 124 NaCl, 3

KCl, 1.3 MgCl, 2.6 $CaCl_2$, 1.25 NaH_2PO_4, 26 $NaHCO_3$, 10 D-glucose; oxygenated with 95% O_2, 5% CO_2). The lumbar spinal column was removed and immersed in ice-cold sucrose aCSF after which the whole lumbar spinal cord was quickly removed via laminectomy. Parasagittal slices were cut at varying thicknesses that excluded gray matter and contained only myelin from the lateral side of the spinal cord. Slices were maintained in aCSF at room temperature (21–23°C) until imaging.

The transmission of light through the myelinated slices was measured using a custom-made laser scanning microscope with a long working distance water immersed objective (40×0.9 NA, LUMPlanFI/IR, Olympus, Japan). Spinal cord slices were illuminated by three laser beams: 473 nm (MBL-FN, Changchun New Industries Optoelectronics Technology, China), 594 nm (Mambo, Cobolt, Sweden) with a typical averaged power of 3 to 4 mW. Imaging was performed by the scanning of the sample placed on a micro controller stage (MPC-200, Sutter Instrument). The 473 nm and 594 nm light was transmitted through the tissue and measured by a photodetector (818 Si Metal Wand Detector, Newport, California, USA) fitted with a 0.8-mm diameter pinhole. The total power of the transmitted light (473 nm and 594 nm) was recorded for different thickness of the sample. The measured transmission was fit with a mono-exponentially decaying curve.

We used a schematic model to estimate the power of light at the fiber tip required to activate opsins in the spinal cord (Figure 3(c)). We assumed an area of $0.5\,\text{mm} \times 0.5\,\text{mm}$ (approximately half a spinal segment in length) on the top of each half of the spinal cord to be irradiated by one-quarter of the output from the diffusive optic fiber tip. We accounted for the reduction in irradiation caused by scattering through myelin with the exponential fit of the empirically measured transmission of light through myelinated slices. We then calculated the power output from the diffusive tip of the optic fiber that would be required to activate opsins in the irradiated area using a threshold of activation (EC_{20}) of $0.3\,\text{mW} \cdot \text{mm}^{-2}$ and $0.75\,\text{mW} \cdot \text{mm}^{-2}$ for ChR2 and ArchT, respectively,[17,18] using the formula:

$$\begin{aligned}\text{Required power (mW)} = {} & EC_{20}(\text{mW} \times \text{mm}^{-2}) \\ & \times \text{irradiated area}\left(\text{mm}^2\right) \\ & \times 4/(\%\ \text{transmission through myelin})\end{aligned}$$

Optogenetic activation

The frequency and intensity of the 488 nm laser (iBeam Smart PT, Toptica Inc, Germany) used for activation of ChR2 was controlled directly through TopControl software (Toptica Inc). The intensity of the 592 nm laser (VFL-P-300-592, MPB Technologies, Montreal, Canada) used for activation of ArchT was controlled with MPB VFL laser software and light delivery was regulated with a custom-made, TTL-controlled acousto-optic modulator (Doric Lenses Inc., Quebec, Canada). Attenuation of the 592 nm laser output below 30 mW was achieved with an in-line, custom-made neutral density filter box (Doric Lenses). All laser output intensities reported refer to light intensity output from a patch cable (200 μm silica core, 0.22 NA, Thor Labs,) used for connection to the epidural optic fiber as measured with a PM100 light meter (Thor Labs).

Mechanical sensitization via peripheral stimulation was induced in fiber implanted $Na_v1.8$-ChR2 mice by stimulating the hind paw of anesthetized mice with 488 nm light at a low frequency (2 Hz, 10 ms pulses) for 20 min as previously described.[5] The light intensity used for peripheral sensitization was 4 to 5 times higher than peripheral threshold intensity. Anesthesia was induced with isoflurane at the minimum concentration required to prevent paw withdrawal from peripheral light stimulus (approximately 1.8%). For epidural activation of ChR2-expressing $Na_v1.8^+$ afferents, the behavioral threshold was determined as the lowest intensity of light delivered via the epidural fiber that produced a behavioral response in the mice, such as twitching, fleeing, or vocalization. The light intensity used for epidural sensitization was 1.5 to 3 times higher than the behavioral threshold, and this intensity induced robust behavioral responses in non-anesthetized mice. Mechanical sensitization was induced in $Na_v1.8$-ChR2 mice with epidural stimulation in anesthetized (1.8% isoflurane) and non-anesthetized mice with 488 nm light at a low frequency (2 Hz, 10 ms pulses) for 20 min. For tests of thermal and mechanical sensitivity using epidural delivery of 592 nm laser light, the laser was activated immediately prior to presentation of each thermal or von Frey stimulus and inactivated immediately after. Each presentation was separated by a minimum of 5 min. Mice were acclimatized to the connection of the patch cable and testing environment for 1 h prior to testing. The various optical approaches used throughout the study are summarized in Table 1.

Behavioral Experiments

Rotarod. Evoked motor performance was tested in naive, fiber-implanted, and non-implanted C57BL/6 mice using a Rotarod (IITC Life Sciences, California, USA). Mice were tested at least two weeks after fiber implantation and all mice were age-matched. Rotation was started immediately after the mice were placed on the rotarod, and accelerated from 0 to 35 RPM over a period of 100 s. The latency to fall was measured and a cut-off time of

100 s was set, but the cut-off was not reached in any trial. Trials were repeated five times per mouse separated by 30 min each.

Novel cage behavior. Spontaneous motor behavior of fiber-implanted and non-implanted C57BL/6 mice was assessed by recording the activity of mice placed in a clean cage fitted with a food hopper, similar to their home cage, but empty of food and water. Mice were tested at least two weeks after fiber implantation and all mice were age-matched. Four mice were tested simultaneously with the experimenter out of the room using and behavior was captured using D-Link 942L network cameras and recorded with iSpy64 software. The mouse behavior and distance traveled by the mice were automatically scored using HomeCageScan software (CleverSys Inc, Virginia, USA) and the time spent in each behavior was totaled. The activity of mice was binned into the behavioral categories of exploration (dig, forage, sniff, rearing), hanging, and resting (no movement) behavior.

Thermal sensitivity. Thermal sensitivity was assessed using a Hargreaves thermal sensitivity apparatus (IITC Life Sciences). Mice were placed on a 3/16th-inch thick glass floor warmed to 29°C within small (8×8 cm) Plexiglas cubicles, and a focused high-intensity projector lamp beam was shone from below onto the mid-plantar surface of the hind paw. For experiments with $Na_v1.8$-ArchT mice, a 715-nm long-pass filter (Thor Labs) was fitted to the projector to avoid activation of peripherally expressed ArchT in nociceptive afferents. Light intensity during stimulation was adjusted to 75% of maximum with the long-pass filter in place. In experiments with GAD2-ArchT mice, the long-pass filter was omitted and stimulation light intensity was set to 20% of maximum. A 30-s withdrawal latency was set, and latency to withdraw from the stimulus was measured to the nearest 0.1 s. Both hind paws were tested twice under each condition and all results were averaged for each experimental condition.

Mechanical sensitivity. Mechanosensitivity was measured using the SUDO up-down method with von Frey hairs to estimate the 50% withdrawal threshold in pressure units ($g \cdot mm^{-2}$).[19] Both hind paws were tested twice under each condition and results were averaged for each experimental condition.

Results

The epidural optic fiber consisted of a length of plastic optical fiber and ceramic ferrule with a small cement base for fixation to the skull (Figure 2(a) and (b)). The length and placement of the fiber was adjusted to ensure the fiber tip was positioned between vertebral spines T13 and L1, corresponding with spinal segments L4 through L6[16] (Figure 2(c)). The optic fiber was terminated in a diffusive tip to enable the diffusion of light ventrally, toward the spinal cord (Figure 3(a)). A diffusive tip design was chosen for this purpose for its combination of robustness and simplicity.

The activation of opsins expressed in afferent fiber terminals and cells of the spinal cord dorsal horn requires light from the optic fiber to pass through the myelinated dorsal surface of the spinal cord, which will scatter light and reduce dorsal horn irradiance. We first measured the transmission of light through various thicknesses of myelin to account for scattering of light by myelin (Figure 3(b)). We found that the degree of scattering is strongly determined by the thickness of myelin and the wavelength of light, with 96% to 99% attenuation of light intensity observed for myelin thicknesses of 50 to 200 μm. We then incorporated these data into a simple model of spinal cord illumination to estimate the total power of light at the fiber tip required to activate spinal cord opsins (Figure 3(c)). We estimated that opsins expressed in afferent fibers that enter the dorsal horn from the dorsal side and are therefore very superficial (<50 μm of myelin) will be activated with a total power output from the tip of the fiber of approximately 5 to 10 mW for ChR2 and 10 to 15 mW for ArchT (Figure 2(d)). Opsins expressed by neurons in the superficial dorsal horn require light to traverse approximately 100 to 150 μm of myelin and therefore require approximately 15 to 35 mW of power output from the tip of the fiber for threshold activation of ChR2, and 25 to 40 mW for threshold activation of ArchT.

The epidural implant was well tolerated in mice, with several mice retaining intact fibers and behavioral responses to epidural light stimulation for up to six months after implantation. To determine whether the epidural optic fiber impaired animal movement, we measured evoked and spontaneous motor performance in the otarod assay and novel cage activity, respectively, of epidural fiber-implanted and non-implanted control mice. In the Rotarod assay, epidural fiber-implanted C57BL/6 mice performed as well as non-implanted controls (Figure 2(e)). Additionally, the total distance traveled as well as the amount of time spent actively exploring, climbing, and resting during a 1-h exposure to a novel home cage environment were similar between implanted and non-implanted mice (Figure 2(f)). These data demonstrate that the epidural fiber implant does not impair evoked or spontaneous motor activity in mice.

Three different optogenetic mouse lines were implanted with the optic fiber: mice expressing ChR2 in $Na_v1.8^+$ nociceptors ($Na_v1.8$-ChR2 mice),[5,13] mice expressing the inhibitory opsin ArchT in $Na_v1.8^+$ nociceptors ($Na_v1.8$-ArchT), and mice expressing ArchT in GABAergic interneurons of the spinal cord dorsal horn

(GAD2-ArchT; Table 1). We first sought to use the epidural optic fiber to activate sensory afferents and induce sensory plasticity in freely behaving $Na_v1.8$-ChR2 mice (Figure 4(a)). The spinal delivery of blue light to $Na_v1.8$-ChR2 mice implanted with the epidural optic fiber produced robust nocifensive behavior (Figure 4(b)). Notably, the mechanical withdrawal threshold of $Na_v1.8$-ChR2 mice did not change after implantation of the fiber compared to preimplantation withdrawal thresholds in the same mice, indicating the fiber implant does not cause mechanical hyperalgesia by itself (Figure 4(c)). Additionally, we confirmed that prolonged, low-frequency peripheral stimulation with blue light (488 nm) applied to the hind paw under anesthesia induced long-lasting mechanical hyperalgesia in epidural fiber-implanted $Na_v1.8$-ChR2 mice as compared to implanted $Na_v1.8$-ChR2 mice mice that received anesthesia but no stimulation (Figure 4(d)).

We next sought to determine whether the prolonged activation of $Na_v1.8$ afferents at the spinal level via the epidural fiber can induce mechanical hypersensitivity. We first tested the effect of epidural stimulation of $Na_v1.8$ afferents in anesthetized mice. Compared to non-stimulated controls, we found that epidural stimulation produced long-lasting mechanical hyperalgesia (Figure 4(e)), similar to that produced by peripheral stimulation of the hind paw. Yet, one advantage of the epidural fiber is the ability to deliver light to the spinal cord of freely behaving (non-anesthetized) animals. We next applied the same low-frequency epidural stimulation paradigm (2 Hz, 20 min) in freely behaving $Na_v1.8$-ChR2 mice and found that a similar hyperalgesia was observed following prolonged epidural light stimulation as compared to non-stimulated controls (Figure 4(f)). The epidural fiber optogenetic paradigm thus enables the stable and well-controlled optogenetic exploration of activity-induced hyperalgesia without the potentially confounding effects of anesthesia.

To demonstrate the ability to optogenetically modulate intrinsic spinal cord circuits with the epidural optic fiber, we used GAD2-ArchT mice (Figure 4(g)) to enable the selective silencing of spinal inhibitory GABAergic interneurons. In these mice, the spinal delivery of orange (592 nm) light with the epidural fiber reduced mechanical withdrawal thresholds (Figure 4(h)). Notably, the power requirements we predicted would be required to activate ArchT within the dorsal horn directly correspond with our behavioral observations for the mechanical hyperalgesia induced by inhibition of GABAergic interneurons. Additionally, the same orange light had no effect on the mechanosensitivity of $Na_v1.8$-ChR2 control mice implanted with the fiber, even though they exhibit nocifensive responses to epidural delivery of blue light, and no behavioral response was seen in implanted C57BL/6 or $Na_v1.8$-ChR2 following the delivery of 592 nm light intensities at up to 200 mW at the fiber tip (data not shown). Of interest, spinal delivery of orange light did not change the thermal sensitivity of GAD-ArchT mice (Figure 4(i)). These findings are consistent with the recent report that the permanent ablation of dynorphin-expressing GABAergic and glycinergic interneurons in the dorsal horn selectively induces hyperalgesia to mechanical but not thermal stimuli.[20] Our results extend these findings by indicating that acute, optogenetic inhibition of inhibitory interneurons in the dorsal horn is sufficient to transiently and reversibly induce mechanical hyperalgesia.

We next tested whether optogenetic inhibition of $Na_v1.8^+$ afferents at the spinal level could effectively suppress nociception. In $Na_v1.8$-ArchT mice with epidural fiber implanted (Figure 4(j)), the acute spinal delivery of orange (592 nm) light prolonged the withdrawal latency to noxious thermal stimulation, demonstrating a suppression of nociception (Figure 4(k)). Conversely, the thermal withdrawal thresholds of epidural-fiber implanted C57BL/6 mice used as controls were not modified by the spinal delivery of orange light up the highest light intensity used, indicating that the spinal delivery of light itself is neither noxious nor analgesic (Figure 4(l)).

Discussion

Overall, these results demonstrate the broad utility of epidural optogenetics for the study and manipulation of sensory afferent and spinal cord sensory network activity. The strategy employed here addresses key limitations of other approaches to sensory optogenetics recently described.[5,6,12] The epidural implant enables the concurrent delivery of any wavelength of light for complete optogenetic control of defined cell populations. The ability to couple the epidural fiber to laser light sources also enables the delivery of sufficiently strong light intensities for the activation of inhibitory opsins such as ArchT as well as the modulation of intrinsic spinal neurons. By extrapolating our irradiance model, we predict that the epidural optic fiber design described here will enable sufficient irradiance for optogenetic manipulation of spinal cord neurons throughout the dorsal horn. As with other methods to deliver light directly to the spinal cord,[12] the epidural optic fiber provides a method for the stable, controlled modulation of sensory afferents in freely behaving animals.[5,8] Yet, because the epidural fiber is uniquely suitable for the activation of inhibitory opsins and the manipulation of intrinsic spinal cord neurons, this approach also enables the use of optogenetics in more complex behavioral assays designed to dissect the integration and processing of sensory inputs.

The transient induction of mechanical but not thermal hyperalgesia upon inhibition of GABAergic neurons

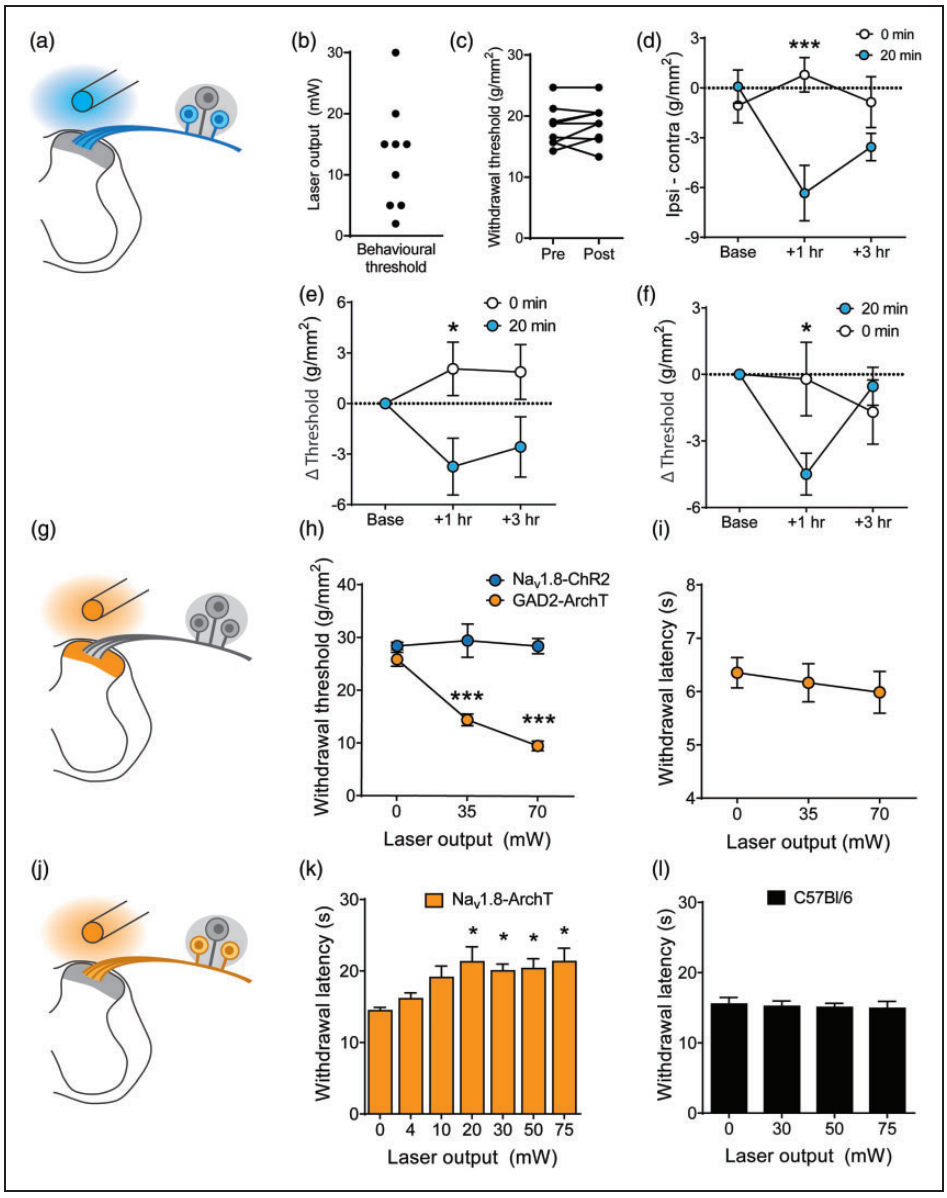

Figure 4. Modulation of nociception through optogenetic control of sensory afferents and spinal cord interneurons. (a) Schematic diagram of optogenetic activation of ChR2-expressing $Na_v1.8^+$ afferents with blue light delivered by epidural optic fiber. (b) Light intensity thresholds for behavioural response of $Na_v1.8$-ChR2 mice to blue light delivered via epidural optic fiber. $n = 9$ mice. (c) Mechanical withdrawal thresholds of $Na_v1.8$-ChR2 mice before (Pre) and after (Post) implantation of the epidural optic fiber. $n = 9$ mice. (d) Reduction of mechanical withdrawal thresholds of $Na_v1.8$-ChR2 mice induced though repetitive stimulation of the hind paw ventral surface with blue light (488 nm) in mice immobilized with anesthesia. $n = 7$ mice per group. (e,f) Reduction of mechanical withdrawal thresholds in $Na_v1.8$-ChR2 mice induced though repetitive epidural optical stimulation with blue light immobilized with anesthesia (e; $n = 5$ mice in 0 min and $n = 6$ mice in 20 min stimulation groups) and in freely-behaving, non-anesthetized animals (*f*; $n = 7$ mice per group). (g) Schematic of optogenetic inhibition of ArchT-expressing GAD2+ inhibitory interneurons in the spinal cord dorsal horn with orange light delivered by epidural optic fiber. (h,i) Reduction of mechanical withdrawal thresholds (*h*; $n = 7$ GAD2-ArchT mice, $n = 3$ $Na_v1.8$-ChR2 mice) but not thermal withdrawal latencies (*i*; $n = 6$ mice) via epidural delivery of orange light in epidural fiber-implanted GAD2-ArchT mice. (j) Schematic of optogenetic inhibition of ArchT-expressing $Na_v1.8^+$ afferents with orange light delivered by epidural optic fiber. (k,l) Reduction of withdrawal latencies to noxious thermal stimulation via delivery of orange (592 nm) light in epidural fiber-implanted $Na_v1.8$-ArchT (*k*; $n = 4$ mice) but not fiber-implanted C57BL/6 mice (*l*; $n = 3$ mice).

parallels results recently obtained through the permanent ablation of somatostatin-positive inhibitory neurons in the dorsal horn.[20] These results, together, suggest that thermal and mechanical hyperalgesia involve different changes in spinal cord sensory processing, with spinal GABAergic disinhibition primarily modulating mechanical sensitivity. However, the temporal fidelity of optogenetics offers a considerable advantage over ablation or pharmacological inhibition approaches to the behavioral studies of spinal cord function.[20,21] In particular, short-term optogenetic silencing avoids possible developmental or compensatory changes that may accompany permanent ablation, as observed in the spontaneous partial recovery of hyperalgesia induced by ablation of spinal cord glycinergic neurons.[22]

Finally, our epidural fiber implant also provides an important demonstration of the utility of epidural optical approaches for possible future use in clinical settings. Chronic, epidural, or intrathecal probes are routinely used for spinal drug delivery or electrical stimulation in pain. While many hurdles still remain, the transfection of peripheral nerves to enable optogenetic control of neuronal activity in humans is a distinct future possibility.[23,24] Our results demonstrate the potential of using epidural or intrathecal optic fibers for the optogentic control of specific sensory afferents as a therapeutic approach for the treatment of sensory disorders in humans.

Conclusions

The epidural optic fiber described here provides a robust and powerful solution for spinal optogenetics that enables activation of both excitatory and inhibitory opsins in sensory processing pathways. Our results demonstrate the potential of spinal optogenetics to modulate sensory behavior and produce analgesia in freely behaving animals.

Author contributions

RPB, FW, MDC, and MEB conducted behavioral and in vitro experiments and analyzed data. RPB, AG, and DCC created and analyzed the physical model of the spinal cord. RPB, FW, AG, DCC, and YDK designed all experiments. RPB, DCC, AG, and YDK wrote the manuscript. All authors reviewed and approved the final manuscript.

Acknowledgments

The authors thank Rohini Kuner for generously providing the $Na_V1.8$-Cre mice; Nicolas Lapointe, Behrang Sharif, and Jimena Perez-Sanchez for their assistance with the figures; Yoan LeChasseur and Anne-Marie Roy for their advice on the design of the optic fiber; and Modesto R. Peralta III for his input on the surgical method.

Declaration of Conflicting Interests

The author(s) declared no potential conflicts of interest with respect to the research, authorship, and/or publication of this article.

Funding

The author(s) disclosed receipt of the following financial support for the research, authorship, and/or publication of this article: This work was supported by a Pfizer-Fonds de recherche Quebec - Sante (FRQS) Innovation Fund Award to YDK, a Canadian Institutes of Health Research grant MOP 12942 to YDK, and the Catherine Bushnell Pain Research Fellowship from the Louise and Alan Edwards Foundation to RPB.

References

1. Todd AJ. Neuronal circuitry for pain processing in the dorsal horn. *Nat Rev Neurosci* 2010; 11: 823–836.
2. Prescott SA, Ma Q and De Koninck Y. Normal and abnormal coding of somatosensory stimuli causing pain. *Nat Neurosci* 2014; 17: 183–191.
3. Braz J, Solorzano C, Wang X, et al. Transmitting pain and itch messages: a contemporary view of the spinal cord circuits that generate gate control. *Neuron* 2014; 82: 522–536.
4. Devor M. Ectopic discharge in Abeta afferents as a source of neuropathic pain. *Exp Brain Res* 2009; 196: 115–128.
5. Daou I, Tuttle AH, Longo G, et al. Remote optogenetic activation and sensitization of pain pathways in freely moving mice. *J Neurosci* 2013; 33: 18631–18640.
6. Iyer SM, Montgomery KL, Towne C, et al. Virally mediated optogenetic excitation and inhibition of pain in freely moving nontransgenic mice. *Nat Biotech* 2014; 32: 274–278.
7. Wang H and Zylka MJ. Mrgprd-expressing polymodal nociceptive neurons innervate most known classes of substantia gelatinosa neurons. *J Neurosci* 2009; 29: 13202–13209.
8. Bonin RP and De Koninck Y. A spinal analog of memory reconsolidation enables reversal of hyperalgesia. *Nat Neurosci* 2014; 17: 1043–1045.
9. Honsek SD, Seal RP and Sandkuhler J. Presynaptic inhibition of optogenetically identified VGluT3+ sensory fibres by opioids and baclofen. *Pain* 2015; 156: 243–251.
10. Hagglund M, Dougherty KJ, Borgius L, et al. Optogenetic dissection reveals multiple rhythmogenic modules underlying locomotion. *Proc Natl Acad Sci USA* 2013; 110: 11589–11594.
11. Wyart C, Del Bene F, Warp E, et al. Optogenetic dissection of a behavioural module in the vertebrate spinal cord. *Nature* 2009; 461: 407–410.
12. Montgomery KL, Yeh AJ, Ho JS, et al. Wirelessly powered, fully internal optogenetics for brain, spinal and peripheral circuits in mice. *Nat Methods* 2015; 12: 969–974.
13. Agarwal N, Offermanns S and Kuner R. Conditional gene deletion in primary nociceptive neurons of trigeminal ganglia and dorsal root ganglia. *Genesis* 2004; 38: 122–129.

14. Shields SD, Ahn HS, Yang Y, et al. $Na_v1.8$ expression is not restricted to nociceptors in mouse peripheral nervous system. *Pain* 2012; 153: 2017–2030.
15. Vrontou S, Wong AM, Rau KK, et al. Genetic identification of C fibres that detect massage-like stroking of hairy skin in vivo. *Nature* 2013; 493: 669–673.
16. Harrison M, O'Brien A, Adams L, et al. Vertebral landmarks for the identification of spinal cord segments in the mouse. *NeuroImage* 2013; 68: 22–29.
17. Han X, Chow BY, Zhou H, et al. A high-light sensitivity optical neural silencer: development and application to optogenetic control of non-human primate cortex. *Front Syst Neurosci* 2011; 5: 18.
18. Lin JY, Lin MZ, Steinbach P, et al. Characterization of engineered channelrhodopsin variants with improved properties and kinetics. *Biophys J* 2009; 96: 1803–1814.
19. Bonin RP, Bories C and De Koninck Y. A simplified up-down method (SUDO) for measuring mechanical nociception in rodents using von Frey filaments. *Mol Pain* 2014; 10: 26.
20. Duan B, Cheng L, Bourane S, et al. Identification of spinal circuits transmitting and gating mechanical pain. *Cell* 2014; 159: 1417–1432.
21. Petitjean H, Pawlowski SA, Fraine SL, et al. Dorsal horn parvalbumin neurons are gate-keepers of touch-evoked pain after nerve injury. *Cell Rep* 2015; 13: 1246–1257.
22. Foster E, Wildner H, Tudeau L, et al. Targeted ablation, silencing, and activation establish glycinergic dorsal horn neurons as key components of a spinal gate for pain and itch. *Neuron* 2015; 85: 1289–1304.
23. Mallory GW, Grahn PJ, Hachmann JT, et al. Optical stimulation for restoration of motor function after spinal cord injury. *Mayo Clin Proc* 2015; 90: 300–307.
24. Williams JC and Denison T. From optogenetic technologies to neuromodulation therapies. *Sci Transl Med* 2013; 5: 177ps6.